Ru(II)-Cyanine Complexes as Promising Photodynamic Photosensitizers for the Treatment of Hypoxic Tumours with Highly Penetrating 770 nm Near-Infrared Light

Albert Gandioso, Eduardo Izquierdo-García, Pierre Mesdom, Philippe Arnoux, Nurikamal Demeubayeva, Pierre Burckel, Bruno Saubaméa, Manel Bosch, Céline Frochot, Vicente Marchán, et al.

HAL Id: hal-04183197

https://hal.science/hal-04183197

Submitted on 18 Aug 2023

Ru(II)-Cyanine Complexes as Promising Photodynamic Photosensitizers for the Treatment of Hypoxic Tumours with Highly Penetrating 770 nm Near-Infrared Light

Dr. Albert Gandioso,[a,*,#] Dr. Eduardo Izquierdo-García,[a,b,#] Dr. Pierre Mesdom,[a] Philippe Arnoux,[c] Nurikamal Demeubayeva,[c] Dr. Pierre Burckel,[d] Dr. Bruno Saubaméa,[e] Dr. Manel Bosch,[f] Dr. Céline Frochot,[c] Prof. Dr. Vicente Marchán[b,*] and Prof. Dr. Gilles Gasser[a,*]

[a] Chimie ParisTech, PSL University, CNRS, Institute of Chemistry for Life and Health Sciences, Laboratory for Inorganic Chemical Biology, F-75005 Paris, France.

[b] Departament de Química Inorgànica i Orgànica, Secció de Química Orgànica, Universitat de Barcelona (UB), and Institut de Biomedicina de la Universitat de Barcelona (IBUB), Martí i Franquès 1-11, E-08028 Barcelona, Spain.

[c] Université de Lorraine, CNRS, LRGP, F-54000 Nancy, France.

[d] Université de Paris, Institut de physique du globe de Paris, CNRS, F-75005 Paris, France

[e] Cellular and Molecular Imaging platform, US25 Inserm, UAR3612 CNRS, Faculté de Pharmacie de Paris, Université Paris Cité, 75006 Paris, France.

[f] Unitat de Microscòpia Òptica Avançada, Centres Científics i Tecnològics, Universitat de Barcelona (CCiTUB), Av. Diagonal, 643, Barcelona, 08028, Spain

# These authors contributed equally to the work

_____

Correspondence:
Albert Gandioso. E-mail: albert.gandioso@chimieparistech.psl.eu
Vicente Marchán. Email: vmarchan@ub.edu
Gilles Gasser. E-mail: gilles.gasser@chimieparistech.psl.eu; WWW. www.gassergroup.com

Abstract

Light-activated treatments, such as photodynamic therapy (PDT), provide temporal and spatial control over a specific cytotoxic response by exploiting toxicity differences between irradiated and dark conditions. In this work, a novel strategy for developing near infrared (NIR)-activatable Ru(II) polypyridyl-based photosensitizers (PSs) was successfully developed through the incorporation of symmetric heptamethine cyanine dyes in the metal complex *via* a phenanthrimidazole ligand. Owing to their strong absorption in the NIR region, the PSs could be efficiently photoactivated with highly penetrating NIR light (770 nm), leading to high photocytotoxicities towards several cancer cell lines under both normoxic and hypoxic conditions. Notably, our lead PS (**Ru-Cyn-1**), which accumulated in the mitochondria, exhibited a good photocytotoxic activity under challenging low-oxygen concentration (2% O_2) upon NIR light irradiation conditions (770 nm), owing to a combination of types I and II PDT mechanism. The fact that the PS Protoporphyrin IX (PpIX), the metabolite of the clinically approved 5-ALA PS, was found inactive under the same challenging conditions positions **Ru-Cyn-1** complex as a promising PDT agent for the treatment of deep-seated hypoxic tumours.

Keywords: cyanine – medicinal inorganic chemistry – photodynamic therapy – photosensitizer – ruthenium(II) complexes

Table of Contents (ToC)

A novel class of Ruthenium(II) complexes that can be photoactivated in hypoxic conditions at 770 nm thanks to the incorporation of heptamethine cyanine dye is described.
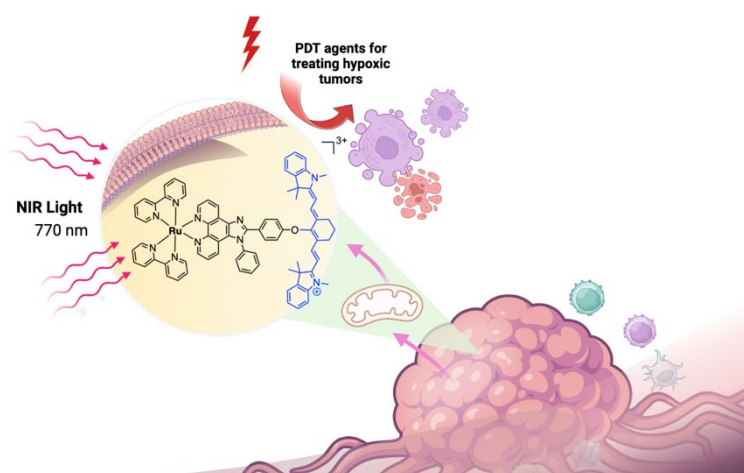
Twitter

@Agandioso , @Eizquiga , @GasserGroup , @ChimieParisTech , @psl_univ , @UniBarcelona @QuimicaUB

Introduction

Cancer remains one of the leading causes of death worldwide[1] and, despite the availability of a wide range of chemotherapeutic drugs in the clinic, the success of current anticancer therapies in achieving cure or prolonged overall survival of patients is often limited by their severe side effects, as well as by the existence of intrinsic or acquired drug resistances.[2–4]

In this context, light holds an enormous potential in cancer therapy since it can be used to control the release of cytotoxic species from an inert, non-toxic drug at a desired time and location. Photodynamic therapy (PDT) and photoactivated chemotherapy (PACT) are two well-established techniques that use light.[5–7] Transition metal complexes and particularly ruthenium(II) polypyridyl complexes have gained attention in recent years as promising photosensitizers (PSs) in anticancer PDT since they can generate highly cytotoxic reactive oxygen species (ROS) upon light irradiation.[8–11] However, very few metal-based PSs operate in the phototherapeutic window (650-900 nm),[12–14] hampering their application in the treatment of large or deep-seated tumours. Besides exhibiting biocompatibility and high penetration depth into human tissues, the use of near-infrared (NIR) light has been widely validated in several clinical applications through numerous optical methods, including *in vivo* fluorescence imaging and fluorescence-guided surgery.[15],[16] Therefore, expansion of the PS toolbox with novel NIR-activatable Ru(II) polypyridyl complexes is expected to enlarge the clinical applications of PDT.[17] To date, to the best of our knowledge, only a reduced number of Ru(II) complexes with operability in the phototherapeutic window have been reported by Therrien (650 nm),[18], McFarland (730 nm)[19,20] and us (740 nm),[21], if we do not take into account two-photon absorption[22,23]. Ideally, (metal-based) PSs should also operate under hypoxic conditions, since solid tumours are characterized by reduced oxygen tension compared with normal tissues, and hypoxia is known to promote tumor angiogenesis, metastasis, and resistance to anticancer chemotherapy, radiotherapy and PDT. This might be a problematic issue in the case of conventional Ru(II) polypyridyl complexes due to the fact that they mainly operate through type II PDT mechanism and, therefore, their photoactivity is highly influenced by intracellular oxygen concentration.

To address all these problems, much effort has been devoted over the last few years to develop novel PSs that join in a single molecule the rich photophysical properties of small organic fluorophores[24,25] and the well-established anticancer activities of transition metal complexes. Some notable examples of this approach include boron-dipyrromethene (BODIPY),[26] coumarin,[27] cyanine,[28,29] or xanthene[30] dyes conjugated to several metal complexes, most of

them cyclometalated Ir(III) complexes. Among organic fluorophores, heptamethine cyanines are particularly interesting since they are currently used in several biomedical applications, as well as in *in vivo* clinical imaging,[31,32] being indocyanine green (ICG) a good example of a NIR fluorescent dye approved by FDA for human clinical applications, including cancer diagnosis.[25]

In this work, we report for the first time Ru(II) polypyridyl complexes with strong absorption in the NIR region owing to the incorporation of a phenanthrimidazole ligand containing a symmetric heptamethine cyanine fluorophore (Phen-Cyn ligand) in the metal coordination sphere (Figure 1). In all cases, a six-membered carbocyclic ring was incorporated in the heptamethine chain to increase the rigidity of the dye molecule, which is known to improve photostability and reduce aggregation in solution.[33,34] As shown in Figure 1, two additional modifications were carried out in **Ru-Cyn-1** to establish a structure-activity relationship (SAR). On the one hand, a iodinated analogue was synthesized (**Ru-Cyn-2**), since the incorporation of heavy iodine atoms into the indoline moieties of the cyanine backbone has been reported to increase the rates of reactive species generation.[35,36] On the other hand, in analogue **Ru-Cyn-3**, the 2,2′-bipyridyl (Bpy) ligands in the Ru(II) complex were replaced by the more lipophilic 4,7-diphenyl-1,10-phenanthroline (bathophenanthroline or Bphen) ligands in order to explore the effect of lipophilicity on the cellular uptake of the PS.[37] The novel PSs exhibited good photoactivity upon irradiation with highly penetrating NIR light (770 nm), both under normoxia and hypoxia conditions owing to the generation of types I and II ROS, which offers new opportunities to combat large and deep-seated solid hypoxic tumours.
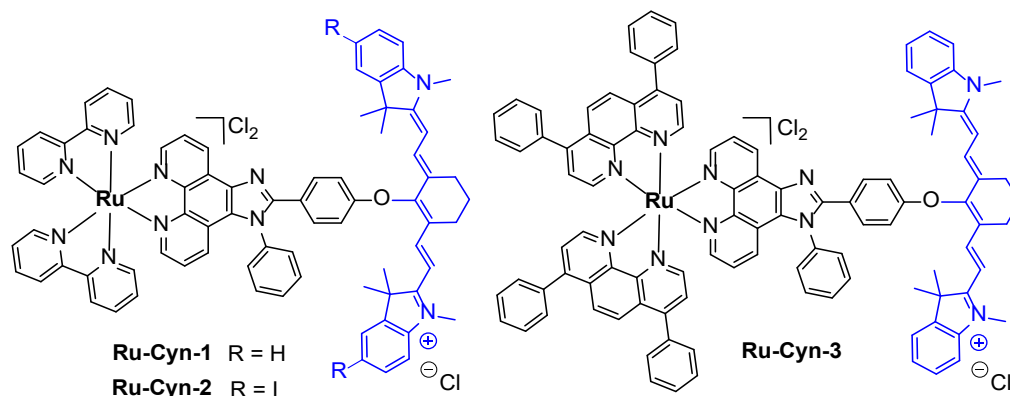

Figure 1. Structures of the ruthenium(II)-cyanine complexes (**Ru-Cyn-1-3**) investigated in this work.

Results and Discussion

First, the required phenanthrimidazole-cyanine ligands (Phen-Cyn **10** and Phen-Cyn-Iodo **11**) were synthesized as indicated in Scheme 1, starting either from commercially available indolinium derivative **4** or from the corresponding iodinated analogue **5**, which was obtained in two steps by reaction of 4-iodophenylhydrazine with 3-methyl-2-butanone to produce the indole intermediate, followed by *N*-methylation with methyl iodide.[38] Aldol-like condensation of the appropriate *N*-methylated indolinium salt and the iminium salt **6** derived from cyclohexanone[39,40] using ethanol as the solvent and sodium acetate as the base afforded the symmetric cyanine derivatives **7** and **8**. In parallel, the imidazole-1,10-phenanthroline (phen) ligand **9** was prepared according to literature procedures.[41,42] Finally, compounds **10** and **11** were satisfactorily obtained by means of a nucleophilic substitution reaction (via an $S_{RN}1$ mechanism)[39,40] of the corresponding chlorocyanine precursors **7** and **8**, respectively, with the *in-situ* generated sodium phenoxide of the phenanthrimidazole derivative **9**.[38,43]
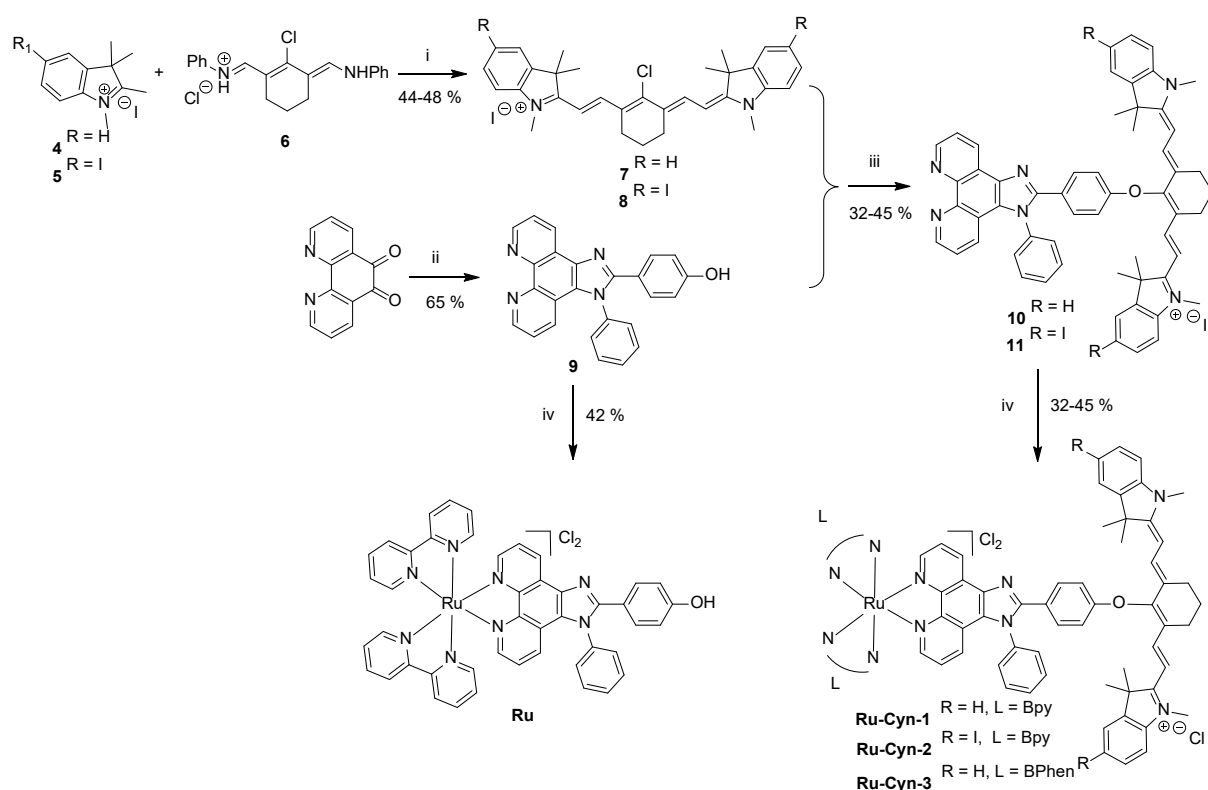
Scheme 1. Synthetic route for the preparation of **Ru-Cyn-1-3** and **Ru**: (i) NaOAc, EtOH, 60 °C, 4 h; (ii) 4-hydroxybenzaldehyde, aniline, NH₄OAc, AcOH, reflux, 15 h; (iii) NaH, DMF, 25 °C, 24 h; (iv) [Ru(Bpy)₂Cl₂] or [Ru(Bphen)₂Cl₂], H₂O/EtOH (1:1, v/v), 70 °C, 15 h.

Having the Phen-Cyn ligands **10** and **11** in hand, the desired **Ru-Cyn-1**–**3** complexes based on the general formula $[Ru(L)_2(Phen-Cyn)]^{3+}$ were easily assembled by reaction with either $[Ru(Bpy)_2Cl_2]$ or $[Ru(Bphen)_2Cl_2]$, which were previously synthesized from $[RuCl_2(DMSO)_4]$ by reaction with the required bidentate ligands (L = Bpy or Bphen) in the presence of an excess of lithium chloride.[44] All the compounds were isolated by silica column chromatography with moderate to good yields and fully characterized by high-resolution ESI mass spectrometry, ^{1}H and ^{13}C-NMR and reversed-phase HPLC analysis, revealing a single peak in all cases.

The photophysical properties of **Ru-Cyn-1-3** complexes were studied in acetonitrile (ACN) and compared with those of the free chlorocyanine (**7**) and of the ruthenium complex lacking the dye (**Ru**), which was synthesized as indicated in Scheme 1. The UV−Vis absorption spectra of the compounds are shown in Figure 2, and their photophysical properties are summarized in Table 1. All Ru(II) complexes display an absorption band around 300 nm in the UV corresponding to Bpy- or Bphen-centered transitions. The less intense bands that appear at ~ 470 nm correspond to the metal-to-ligand charge transfer (MLCT) transitions that involve both the metal center and the ligands. Importantly, all the Ru-Cyn complexes showed an intense absorption band in the NIR region of the electromagnetic spectrum owing to the coordination of the Phen-Cyn ligand, being the absorption maxima dependent on the cyanine dye (e.g. λ_{abs} = 766 nm for **Ru-Cyn-1** and λ_{abs} = 779 nm for **Ru-Cyn-2**).
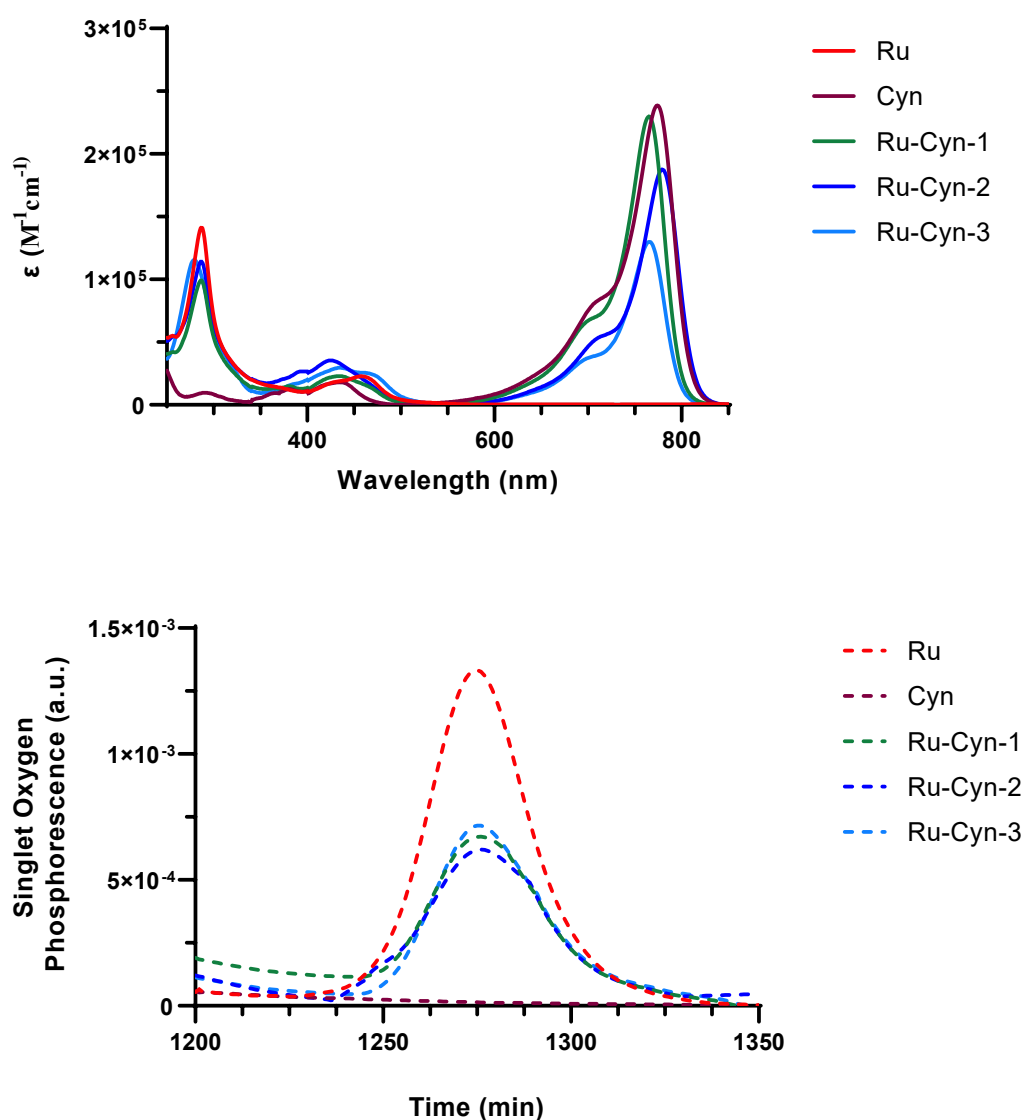
Figure 2. UV-Vis absorption spectra (Top) and singlet oxygen ($^1O_2$) emission spectra (λ_{ex} = 450 nm) (Bottom) of the compounds measured in acetonitrile.

Additionally, **Ru-Cyn-1-3** showed emission in the NIR region upon excitation on the MLCT band at 450 nm (Figure S1), with maximum emission wavelengths ranging from 796 nm (**Ru-Cyn-1**) to 809 nm (**Ru-Cyn-2**), which demonstrated that the incorporation of the cyanine dye into the phenanthrimidazole ligand was highly positive to red-shift both absorption and emission of the resulting Ru(II) polypyridyl complex into the phototherapeutic window. As indicated in Table 1, the phosphorescence quantum yield of the ruthenium complex **Ru** was significantly higher than those of the Ru-Cyn complexes, which suggests the presence of light-promoted reactions upon light irradiation. The lifetimes of this ^{3}MLCT state are in the range of 150-200 ns for **Ru-cyn-1-3** in degassed ACN in excitation of 407 nm. Also, it exhibited a bi-

exponential decay with a short lifetime attributed to the cyanine dye and a long one between 150 and 200 ns due to the Ru complex.

Table 1. Photophysical properties and singlet oxygen quantum yield of the compounds. (Φ_P = phosphorescence quantum yield, τ_P= Ru complex lifetime of ^{3}MLCT state, Φ_Δ= $^1O_2$ quantum yield).

	λ_{abs} (nm)	λ_{em} (nm)	Stokes' shift (nm)	Φ_P (%)	τ_P (ns)	Φ_Δ (%)
Ru	458	607	--	10	189	86
Ru-Cyn-1	766	796	30	1	202	21
Ru-Cyn-2	779	809	30	1	172	20
Ru-Cyn-3	765	805	30	1	149	27

Since $^1O_2$ is the main cytotoxic species produced by Ru(II)-based PSs operating through type II PDT mechanism, we focused on the quantification of the amount of $^1O_2$ generated upon irradiation of the compounds at the MLCT band (λ_{exc} = 450 nm) by measuring the phosphorescence produced by the relaxation of $^1O_2$ (λ_{em}= 1275 nm) in degassed ACN as a function of the irradiation time (Figure 2).[45,46] The $^1O_2$ quantum yield was calculated using [Ru(bpy)$_3$]Cl$_2$ (Φ_Δ = 57% in air-equilibrated ACN)[47] as a standard. As shown in Table 1, **Ru-Cyn-1** and **Ru-Cyn-2** were able to sensitize $^1O_2$ at a similar level, which indicates that the incorporation of two iodine atoms in the cyanine ligand was not sufficient to influence this property. In contrast, the replacement of Bpy with Bphen had a positive effect on singlet oxygen generation (complex **Ru-Cyn-3**). As expected, cyanine **7** did not generate singlet oxygen upon light irradiation (Φ_Δ < 1 %, data not shown), which is in agreement with the low singlet oxygen quantum yield reported for other heptamethine cyanine dyes such as indocyanine green (Φ_Δ = 7 %).[25,32]

Ru-Cyn-1 was then chosen as a representative Ru-cyanine complex to evaluate its stability in biologically-relevant medium, both in the dark and upon irradiation with deep-red light by RP-HPLC analysis. No significant degradation of **Ru-Cyn-1** (~ 6%) was observed after incubation in DMEM medium (Gibco) for 24 h at 37 °C, demonstrating high stability in the dark (Figure S2 and Figure S3). However, upon deep-red light irradiation (650-centered LED, 95 mW/cm^2) for 1 h, **Ru-Cyn-1** underwent a considerable photodegradation (~60%), which resembles the behavior of similar polymethine-containing cyanine fluorophores.[48] (Figure S2 and Figure S4).

The intracellular uptake of the Ru-Cyn complexes was studied by both inductively-coupled plasma mass spectrometry (ICP-MS) and fluorescence microscopy (Figure 3). Since lipophilicity strongly influences both the cellular uptake and subcellular localization of a given bioactive molecule, we first determined the distribution coefficients between octanol and water ($\log P_{O/W}$) of compounds **Ru-Cyn-1**, **Ru-Cyn-2** and **Ru-Cyn-3** (Table S1 and Figure S5). The $\log P_{O/W}$ values followed the order **Ru-Cyn-1** (–0.37) < **Ru-Cyn-2** (+0.03) < **Ru-Cyn-3** (+0.37), indicating that a considerable amount of the PS was found in the water layer, even in the case of the relatively hydrophobic Bphen analogue **Ru-Cyn-3**.
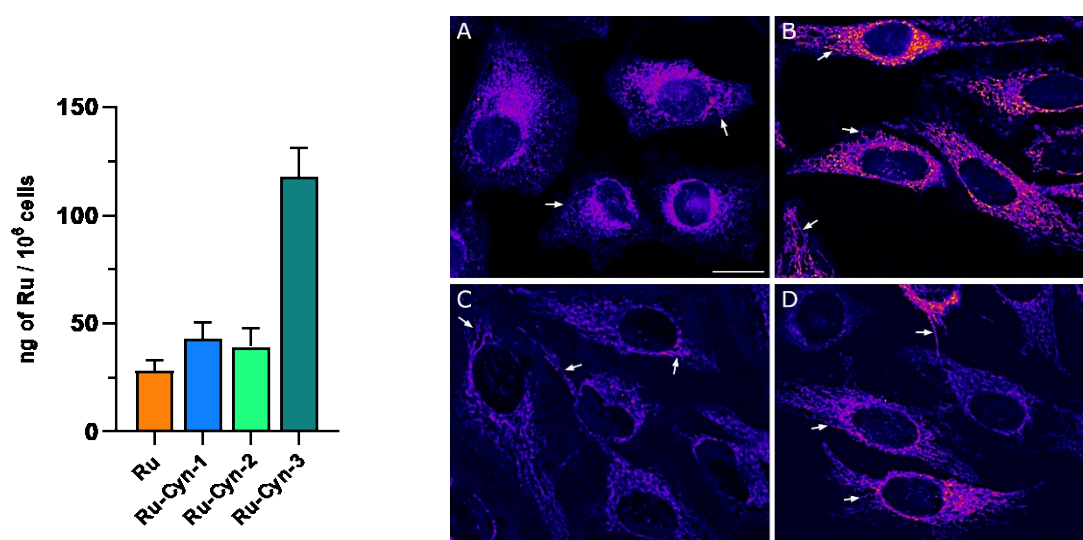

Figure 3. Cellular uptake of the studied compounds. Left: Intracellular accumulation of Ru(II) complexes **Ru**, **Ru-Cyn-1**, **Ru-Cyn-2** and **Ru-Cyn-3** in CT-26 cells after 4 h treatment at 10 μM. Right: Optical sections of HeLa cells treated for 1 h at 37ºC with the compounds **Cyn 7** (A), **Ru-Cyn-1** (B), **Ru-Cyn-2** (C) and **Ru-Cyn-3** (D) at 10 μM, after excitation at 730 nm. Fluorescent signal is shown in Fire LUT. Arrows point out elongated mitochondria. Scale bar = 20 μm.

The cellular uptake of **Ru-Cyn-1-3** complexes, as well as that of **Ru**, was investigated in mouse colon carcinoma cells (CT-26) by quantifying the intracellular amount of metal after 4 h of incubation at 10 μM using inductively coupled plasma mass spectrometry (ICP-MS) (Figure 3, left). **Ru-Cyn-3** was found to have the highest cellular accumulation, which could be attributed to the higher lipophilicity of the Bphen ligand compared with Bpy. Nevertheless, it is worth noting that Ru accumulation from **Ru-Cyn-1** and **Ru-Cyn-2** was slightly higher than that of the control Bpy complex lacking the cyanine ligand (**Ru**), thereby suggesting that the cyanine dye might also favor cellular uptake. Taking advantage of the luminescence emission in the

NIR region of the electromagnetic spectrum of the cyanine dye, the internalization of **Ru-Cyn-1**, **Ru-Cyn-2** and **Ru-Cyn-3** complexes, as well as that of free **Cyn 7**, could be easily tracked in living human cervix adenocarcinoma (HeLa) cells by fluorescence microscopy upon excitation with a 730 nm LED, being the emission detected from 770 to 850 nm. After 1 h incubation, in all cases, the luminescence signal could be detected inside the cell (Figure 3, right), confirming that both the free cyanine and the Ru-Cyn complexes were rapidly and efficiently internalized in cancer cells. Furthermore, across the four studied compounds, a clear filamentous staining pattern was observed, which is highly indicative of mitochondrial accumulation.[49] In order to confirm the subcellular localization of the studied compounds, we performed co-localization experiments in HeLa cells (Figure 4 and Figure S6) using a specific marker for mitochondria (MitoTracker Green). As shown in Figure 4, the luminescence emission of **Ru-Cyn-1** and that of MTG displayed superimposable distributions, leading to a relatively high Pearson's correlation coefficient value (PCC = 0.76), thus, confirming that **Ru-Cyn-1** accumulates preferentially in the mitochondria. Comparable results were obtained in colocalization experiments between **Cyn 7** (Figure 4), **Ru-Cyn-2** or **Ru-Cyn-3** and MTT (Figure S6, Table S2, PCC = 0.74, 0.67 and 0.69, respectively). Overall, fluorescence microscopy studies revealed that the incorporation of a cyanine fluorophore in the ruthenium(II) polypyridyl complex not only pushes the absorption maximum into the desired NIR region but also leads to a preferential accumulation of the complex in the mitochondria, regardless of the structural modifications incorporated either at the cyanine dye (**Ru-Cyn-2**) or at the Ru(II) polypyridyl complex (**Ru-Cyn-3**). These results are not surprising, since heptamethine cyanine dyes have already been reported to target mitochondria.[49] This can be explained by the fact that molecules combining lipophilic and cationic moieties often display a certain mitochondrial targeting specificity due to the negative potential across the outer and inner mitochondrial membrane.[50] Mitochondria are involved in many relevant cellular functions including bioenergy production, control of the homeostasis of intracellular Ca^{2+} levels and oxidative stress, and play a capital role in the regulation of many cell death pathways including apoptosis, cell necrosis and autophagy.[51] Mitochondrial malfunction and dysfunction often result in cell death. In this sense, conjugation to mitochondria-targeting groups has been reported to enhance the cytotoxicity of anticancer drugs.[49] Moreover, mitochondria have been found to be a crucial subcellular target for many PSs used in PDT, since many PSs are able to induce apoptosis by means of mitochondrial damage upon irradiation.[51]
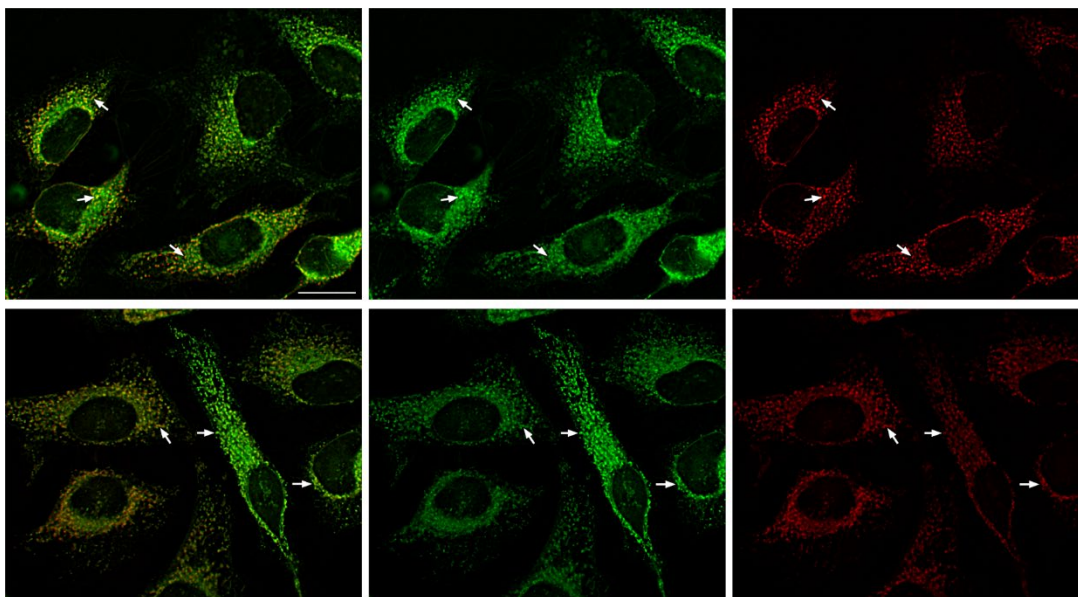
Figure 4. Colocalization studies of **Cyn 7** and **Ru-Cyn-1** with Mitotracker Green. Optical section of HeLa cells treated for 1 h at 37 °C with 10 μM **Cyn 7** (top) and 10 μM **Ru-Cyn-1** (bottom) and 30 min with MTG. Left: merged images; center: MTG signal; right: compound signal. Arrows point out some colocalizing mitochondria. Scale bar = 20 μm.

Once demonstrated that **Ru-Cyn-1-3** complexes display an appropriate internalization in living cancer cells and are able to sensitize singlet oxygen, we next investigated their photocytotoxicity in monolayer cultures of cancer cells upon irradiation with NIR light, taking advantage of their strong absorption in this region of the electromagnetic spectrum. The first screening was carried out in CT-26 cells upon irradiation at 740 nm (Table 2) and revealed that **Ru-Cyn-1** was phototoxic in the low micromolar concentration range ($IC_{50} = 0.17 \pm 0.03$ μM). Although **Ru-Cyn-1** was also found slightly toxic in the absence of light treatment ($IC_{50} = 18.14 \pm 1.10$ μM), the compound still showed a good phototherapeutic index (PI = 106), *i.e.* the ratio of the IC_{50} value in the dark to the IC_{50} value upon irradiation. The iodinated analog **Ru-Cyn-2** exhibited similar photoactivity upon irradiation at 740 nm ($IC_{50} = 0.15 \pm 0.05$ μM) but the higher toxicity in the dark ($IC_{50} = 1.10 \pm 0.08$ μM) resulted in a much smaller PI value (7). Surprisingly, **Ru-Cyn-3** was found less photocytotoxic (IC_{50}, 740 nm $= 1.54 \pm 0.60$ μM; IC_{50}, dark $= 5.00 \pm 0.08$ μM; PI = 3) despite the higher cellular accumulation according to ICP-MS results and higher $^1O_2$ quantum yield when compared with compounds **1** and **2**.

Table 2. IC_{50} values (μM) in normoxic conditions, in the dark and upon irradiation at 740 nm for the investigated compounds towards CT-26 cells.[a] Average of three independent measurements.

		Dark	**740nm**	
		IC_{50}	IC_{50}	PI^b
Ru-Cyn-1	Normoxia	18.14 ± 1.10	0.17 ± 0.03	106
Ru-Cyn-2	Normoxia	1.10 ± 0.08	0.15 ± 0.05	7
Ru-Cyn-3	Normoxia	5.00 ± 0.08	1.54 ± 0.60	3

[a]Cells were treated for 4 h and exposed to light irradiation for 1 h followed by 24 h recovery period. Light irradiation: 740 nm (spectral half-width: 32 nm, 60 min, 3.50 mW cm^{-2}, 12.6 J cm^{-2}). Dark analogues were kept in the dark.

[b]PI = Phototherapeutic index defined as [IC_{50}] dark / [IC_{50}] light

In light of these results, **Ru-Cyn-1** was selected as the most promising PS of the study and we further evaluated its photocytotoxicity towards various cancer cell lines upon irradiation with deep-red light (645 nm) and NIR light (770 nm), both under normoxic (21 % O_2) and hypoxic (2 % O_2) conditions (Table 3). Protoporphyrin IX (PpIX), the metabolite of the clinically approved 5-ALA PS, was also tested for comparative purposes. To our delight, under normoxic conditions (21 % O_2), **Ru-Cyn-1** showed a high photocytotoxicity towards CT-26 cancer cells upon irradiation with both 645 nm and 770 nm light ($IC_{50}(645) = 0.57 \pm 0.24$ µM; $IC_{50}(770) = 0.33 \pm 0.24$ µM), leading to moderate phototherapeutic indices (PI(645) = 32; PI(770) = 55). While PpIX was very phototoxic upon irradiation with 645 nm light and showed a remarkable PI (> 588), as a result of its reduced dark toxicity compared to the **Ru-Cyn** complexes, it was found completely inactive upon irradiation with 770 nm light, due to its lack of absorption beyond 700 nm (Figure S1).[52]

Table 3. IC_{50} values (µM) in normoxic (N, 21 % O_2) and hypoxic (H, 2 % O_2) conditions, in the dark and upon irradiation at 645 nm and 770 nm for the investigated compounds towards CT-26 cells.[a] Average of three independent measurements.

		Dark	**645nm**			**770nm**		
		IC_{50}	IC_{50}	PI^b	HI^c	IC_{50}	PI^b	HI^c
Ru	Normoxia	>100	>100	1	---	>100	1	---
Cyanine 7	Normoxia	0.20 ± 0.05	0.36 ± 0.03	0.55	----	0.63 ± 0.02	0.32	---
Ru-Cyn-1	Normoxia	18.14 ± 0.07	0.57 ± 0.24	32	1.3	0.33 ± 0.24	55	1.8
	Hypoxia	12.03 ± 0.30	0.75 ± 0.10	16		0.62 ± 0.04	20	
PpIX	Normoxia	>100	0.17 ± 0.21	>588	4.7	>100	1	---
	Hypoxia		0.81 ± 0.01	>123				

^{a}Cells were treated for 4 h and exposed to light irradiation for 1 h followed by 24 h recovery period. Light irradiation: 645 nm (spectral half-width: 32 nm, 60 min, 2.50 mW cm^{-2}, 9.0 J cm^{-2}) and 770 nm (spectral half-width: 32 nm, 60 min, 6.75 mW cm^{-2}, 24.3 J cm^{-2}). Dark analogues were kept in the dark.
^{b}PI = Phototherapeutic index defined as [IC$_{50}$] dark / [IC$_{50}$] light
^{c}HI = Hypoxia index defined as [IC$_{50}$] hypoxia/[IC$_{50}$] normoxia

Very importantly, **Ru-Cyn-1** retained a considerable photocytotoxicity towards CT-26 cells under low oxygen concentration (2%) conditions even upon irradiation with 770 nm light (IC$_{50}$ = 0.62 ± 0.04 μM). To the best of our knowledge, this is the first Ru(II) polypyridyl complex reported to be active at 770 nm upon one-photon irradiation, both under normoxia and hypoxia. As shown in Table 3, upon irradiation at 645 nm, a smaller hypoxia index (HI), defined as the ratio from light IC$_{50}$ in normoxia to hypoxia, was found for **Ru-Cyn-1** (HI = 1.3) than for PpIX (HI = 4.7)[53]. This indicates that the photoactivity of the Ru-Cyanine PS is much less influenced by oxygen concentration than that of PpIX. A similar behaviour was found upon irradiation at 770 nm light (HI = 1.8), where PpIX was found to be non-active. The photodynamic threshold dose (T$_{LD50}$), *i.e.* the photon density absorbed by a PS responsible for causing 50 % cell kill, of all the **Ru-Cyn** PSs was calculated according to the method described by Lilge, McFarland and co-workers.[9] (Table S3). Notably, **Ru-Cyn-1** and **Ru-Cyn-2** exhibited relatively low T$_{LD50}$ values (T$_{LD50}$(**Ru-Cyn-1**, 645 nm) = 3.38 x 10^{17}; T$_{LD50}$(**Ru-Cyn-2**, 740 nm) = 5.12 x 10^{17}), indicating a high quantum efficacy for inducing cell death, which usually results from the combination of a high cellular uptake, high level of ROS production and/or the generation of ROS at sensitive cellular targets, such as the mitochondria.[9] Interestingly, **Ru-Cyn-1** was also found to be highly photocytotoxic towards other cancer cell lines including human colon cancer cells (HT-29) and cervical cancer cells (A-2780) upon irradiation at 770 nm under normoxic conditions (IC$_{50}$ = 0.12 ± 0.24 μM, PI = 101 and IC$_{50}$ = 0.08 ± 0.01 μM, PI = 137, respectively).

The operability of **Ru-Cyn-1** PS under low oxygen conditions suggests that singlet oxygen might not the principal cytotoxic ROS being generated. In order to better understand the PDT mechanism by which **Ru-Cyn-1** induces cell death, we next studied the nature of the ROS generated upon irradiation of the PS. In this context, we evaluated the generation of singlet oxygen, hydroxyl radical and superoxide anion radical by **Ru-Cyn-1** upon irradiation with deep-red (645-centered) light using commercially available fluorogenic probes that are specific to each ROS. On the one hand, we used Singlet Oxygen Sensor Green (SOSG) to further confirm the generation of singlet oxygen. On the other hand, the photogeneration of hydroxyl radical and superoxide anion radical were assessed using hydroxyphenyl fluorescein (HPF) and

dihydrorhodamine 123 (DHR123), respectively. As shown in Figure S16, in all cases, an increase of fluorescence intensity of the probe was observed upon irradiation of **Ru-Cyn-1** with deep-red light. Furthermore, the enhancement of fluorescence signal by the different ROS-specific probes could be prevented using appropriate ROS-specific scavengers. All these results confirmed that **Ru-Cyn-1** is able to promote the generation of both Type I (hydroxyl and superoxide radicals) and Type II (singlet oxygen) ROS, which explains its high phototoxicity even under severe hypoxic conditions. Since the PDT response of conventional PSs is reduced when the oxygen supply is low, the availability of light-responsive metal complexes that exploit oxygen-independent phototoxic pathways to maintain efficacy under hypoxia offers new opportunities to combat some of the most aggressive and drug-resistant hypoxic tumors.[12,27,54–58]

Conclusions

In summary, a novel strategy for developing NIR-activatable Ru(II)-based PSs was successfully developed through incorporation of a phenanthrimidazole ligand containing symmetric heptamethine cyanine fluorophores in the metal coordination sphere. Importantly, the strong luminiscence emission of the heptamethine cyanine dye allowed us to confirm the efficient cellular uptake of the three Ru-Cyn PSs and their preferential accumulation in the mitochondria. Owing to their strong absorption in the NIR region, Ru-Cyanine PSs were efficiently photoactivated with highly penetrating NIR light. In particular, **Ru-Cyn-1** exhibited IC_{50} values in the submicromolar range across a panel of cancer cell lines upon irradiation with NIR (770 nm) light. Very importantly, **Ru-Cyn-1** retained a good photocytotoxic activity under challenging hypoxic conditions (2% O_2) upon irradiation with NIR (770 nm) light, in which the reference PS PpIX was found to be inactive, which position such complexes as promising candidates for the treatment of deep-seated hypoxic tumours. The ability of **Ru-Cyn-1** to operate under hypoxia could be attributed to the ability of the compound to photogenerate highly cytotoxic type I ROS (hydroxyl radical and superoxide anion radical) in addition to type II singlet oxygen. Work is in progress in our laboratory to develop novel Ru-cyanine analogues with improved photostability through the incorporation of constrained cyanine dyes with the aim of using them in *in vivo* NIR PDT experiments.

Experimental Section

Materials

All chemicals were either reagent or analytical grade and were purchased from commercial sources without additional purification. All solvents were of analytical, or HPLC grade. When necessary, solvents were degassed by purging with dry, oxygen-free nitrogen for at least 30 min before use. Ruthenium precursors [Ru(DMSO)$_4$Cl$_2$], [Ru(Bpy)$_2$Cl$_2$] and [Ru(Bphen)$_2$Cl$_2$] were prepared according to previously reported procedures.[59,60]

Instrumentation and methods

Schlenk glassware and a vacuum line were employed when reactions sensitive to oxygen had to be performed under nitrogen atmosphere. Thin layer chromatography (TLC) was performed using silica gel 60 F-254 (Merck) plates with detection of spots being achieved by exposure to UV light. Column chromatography was done using Silica gel 60-200 μm (VWR). Eluent mixtures are expressed as volume to volume (v/v) ratios. ^{1}H and ^{13}C NMR spectra were measured on Bruker Advance III HD 400 MHz or Bruker Advance Neo 500 MHz spectrometers using the signal of the deuterated solvent as an internal standard. The chemical shifts (δ) are reported in ppm (parts per million) relative to tetramethylsilane (TMS) or signals from the residual protons of deuterated solvents. Coupling constants J are given in Hertz (Hz). The abbreviation for the peaks multiplicity is s (singlet), d (doublet), dd (doublet of doublet), m (multiplet). ESI-HRMS experiments were carried out using a LTQ-Orbitrap XL from Thermo Scientific (Thermo Fisher Scientific, Courtaboeuf, France) and operated in positive ionization mode, with a spray voltage at 3.6 kV. Sheath and auxiliary gas were set at a flow rate of 5 and 0 arbitrary units (a.u.), respectively. The voltages applied were 40 and 100 V for the ion transfer capillary and the tube lens, respectively. The ion transfer capillary was held at 275°C. Detection was achieved in the Orbitrap with a resolution set to 100,000 (at m/z 400) and a m/z range between 200-2000 in profile mode. Spectrum was analyzed using the acquisition software XCalibur 2.1 (Thermo Fisher Scientific, Courtaboeuf, France). The automatic gain control (AGC) allowed the accumulation of up to 2.105 ions for FTMS scans, Maximum injection time was set to 300 ms, and 1 μscan was acquired. 5 μL was injected using a Thermo Finnigan Surveyor HPLC system (Thermo Fisher Scientific, Courtaboeuf, France) with a continuous infusion of methanol at 100 μL min^{-1}. The absorption of the samples was measured with a Cytation 5 microplate reader (Agilent BioTek). Analytical HPLC measurement was performed using the 2 x Agilent G1361 1260 Prep Pump system with Agilent G7115A1260 DAD WR Detector equipped with an Agilent Pursuit XRs 5C18 (100 Å, C18 5 μm 250 x 4.6 mm) column and an Agilent G1364B 1260-FC fraction collector. The solvents (HPLC grade) were CH$_3$CN (0.1% TFA, solvent A) and Millipore water (0.1% TFA, solvent B). The flow rate was 1

mL/min. Detection was performed at 215 nm, 250 nm, 350 nm, 450 nm, 550 nm, and 650 nm with a slit of 4 nm.

Synthesis and Characterization of Cyanine Ligands (10-11)

5-Iodo-1,2,3,3-tetramethyl-3H-indol-1-ium iodide (Compound 5).

This compound was prepared by adaptation of a reported procedure.[38] A stirred solution of 4-iodophenylhydrazine (2.00 g, 8.53 mmol) and 3-methyl-2-butanone (1.25 g, 14.50 mmol) in EtOH (50 mL) containing a catalytic amount of H_2SO_4 (128 μL, 1.36 mmol) was refluxed for 4 h under a N_2 atmosphere. After cooling to room temperature, the reaction mixture was neutralised with a saturated aqueous solution of Na_2CO_3 until pH~7.0. The mixture was diluted with water (50 mL) and extracted with DCM (4x30 mL). The combined organic extracts were dried over anhydrous $MgSO_4$, filtered and the solvent was evaporated under reduced pressure to give a red oil. The oil was dissolved in ACN (60 mL), treated with iodomethane (663 μL, 10.65 mmol) and the resulting mixture was stirred for 15 h at 85 °C under a N_2 atmosphere. After the reaction mixture was cooled to room temperature, an orange precipitate appeared that was collected by filtration, washed with cold Et_2O, and dried under vacuum to yield crude compound **5** as an orange powder (1.3 g, 37 % yield, over 2 steps) that was used in the following step without any further purification.

TLC: R_f (5 % MeOH in DCM) 0.22.

^{1}H NMR (400 MHz, DMSO-d_6) δ 8.28 (d, J = 1.5 Hz, 1H), 8.00 (dd, J = 8.4, 1.6 Hz, 1H), 7.71 (d, J = 8.3 Hz, 1H), 3.92 (s, 3H), 2.72 (s, 3H), 1.51 (s, 6H).

HRMS (ESI-TOF) *m/z* [M]$^+$ calcd for $C_{12}H_{15}NI$ 300.0244, found 300.0241.

Compound 7.

This compound was prepared by adaptation of a reported procedure.[39,40] A solution of 1,2,3,3-tetramethyl-3*H*-indolium iodide (1.01 g, 3.36 mmol), *N*-((2-chloro-3-((phenylimino)methyl)cyclohex-2-en-1-ylidene)methyl)aniline hydrochloride (550 mg, 1.53 mmol) and NaOAc (501 mg, 6.12 mmol) in EtOH (50 mL) was stirred for 4 h at 60 °C under a N_2 atmosphere. The solvent was concentrated *in vacuo* and the crude was purified by column chromatography (silica gel, 0-10% MeOH in DCM) to give compound **7** (450 mg, 48 % yield) as a dark blue solid.

TLC: R_f (5 % MeOH in DCM) 0.32.

¹H NMR (400 MHz, CD₃CN) δ (ppm): 8.38 (d, *J* = 14.2 Hz, 2H), 7.50 (d, *J* = 7.6 Hz, 2H), 7.43 (td, *J* = 7.8, 1.2 Hz, 2H), 7.28 (td, *J* = 8.0, 0.9 Hz, 4H), 6.19 (d, *J* = 14.3 Hz, 2H), 3.59 (s, 6H), 2.70 (t, *J* = 5.8 Hz, 4H), 1.99 – 1.92 (m, 2H), 1.70 (s, 12H).

Compound 8.

This compound was prepared by adaptation of a reported procedure.[39,40] A solution of 2,3,3-tetramethyl-5-iodo-3*H*-indolium iodide (750 mg, 1.75 mmol), *N*-((2-chloro-3-((phenylimino)methyl)cyclohex-2-en-1-ylidene)methyl)aniline hydrochloride (300 mg, 0.83 mmol) and NaOAc (340 mg, 4.17 mmol) in EtOH (50 mL) was stirred for 4 h at 60 °C under a N₂ atmosphere. The solvent was concentrated *in vacuo* and the crude was purified by column chromatography (silica gel, 0-5% MeOH in DCM) to give compound **8** (320 mg, 44 % yield) as a dark blue solid.

TLC: R_f (5 % MeOH in DCM) 0.38.

¹H NMR (400 MHz, DMSO-*d₆*) δ 8.23 (d, J = 14.3 Hz, 1H), 8.03 (d, J = 1.6 Hz, 1H), 7.83 – 7.71 (m, 2H), 7.59 (dd, J = 8.3, 1.8 Hz, 1H), 7.27 (d, J = 8.4 Hz, 1H), 7.27 – 7.18 (m, 1H), 6.94 (d, J = 8.4 Hz, 1H), 6.29 (d, J = 14.2 Hz, 1H), 5.64 (d, J = 13.0 Hz, 1H), 3.65 (s, 3H), 3.55 (s, 3H), 2.71 (t, J = 5.9 Hz, 2H), 2.60 (t, J = 6.8 Hz, 2H), 1.90 – 1.81 (m, 1H), 1.81 – 1.71 (m, 1H), 1.66 (s, 6H), 1.55 (s, 6H).

HRMS (ESI-TOF) *m/z* [M]⁺ calcd for $C_{32}H_{34}ClN_2I_2$= 735.0494, found 735.0502.

Compound 9.

This compound was prepared by adaptation of a reported procedure.[41,42] A stirred solution of 1,10-phenanthroline-5,6-dione (500 mg, 2.37 mmol), ammonium acetate (2.20 g, 28.55 mmol), aniline (266 mg, 2.85 mmol) and *p*-hydroxybenzaldehyde (290 mg, 2.38 mmol) in glacial AcOH (25 mL) was refluxed for 15 h under a N₂ atmosphere. After cooling to room temperature, the reaction mixture (red solution) was diluted with water (30 mL) and neutralised with a 28% aq. NH₄OH solution until pH~6. The resulting thick dark green suspension was extracted with chloroform (3x30 mL), the combined organic extracts were dried over anhydrous MgSO₄, filtered, and the solvent was concentrated *in vacuo* to give compound **9** (600 mg, 65% yield) as an off-yellow solid.

¹H NMR (400 MHz, DMSO-*d₆*) δ 9.85 (s, 1H), 9.07 (dd, J = 4.3, 1.8 Hz, 1H), 9.00 (dd, J = 8.1, 1.8 Hz, 1H), 8.92 (dd, J = 4.2, 1.7 Hz, 1H), 7.86 (dd, J = 8.1, 4.3 Hz, 1H), 7.71 (s, 5H),

7.46 (dd, J = 8.4, 4.3 Hz, 1H), 7.40 (d, J = 8.7 Hz, 2H), 7.32 (dd, J = 8.4, 1.7 Hz, 1H), 6.71 (d, J = 8.7 Hz, 2H).

HRMS (ESI-TOF) *m/z* [M+H]$^+$ calcd for $C_{25}H_{17}N_4O$ = 389.1397, found 389.1397.

Compound 10.

To a stirred solution of compound **9** (150 mg, 0.38 mmol) in anhydrous DMF (10 mL), under a N_2 atmosphere, was added NaH (20 mg, 0.38 mmol). After stirring for 10 min at room temperature, a solution of compound **7** (230 mg, 0.38 mmol) in anhydrous DMF (5 mL) was added dropwise and the resulting mixture was stirred for another 24 h at room temperature under a N_2 atmosphere. The solvent was removed *in vacuo* and the crude mixture was purified by column chromatography (silica gel, 0-20% MeOH in DCM) to afford compound **10** (150 mg, 45 % yield) as a dark blue solid.

TLC: R_f (10 % MeOH in DCM) 0.12.

^{1}H NMR (400 MHz, CD$_3$CN) δ (ppm): δ 9.08 (dd, J = 4.3, 1.8 Hz, 1H), 9.01 (dd, J = 8.1, 1.8 Hz, 1H), 8.93 (dd, J = 4.1, 1.8 Hz, 1H), 7.84 (d, J = 14.3 Hz, 2H), 7.79 (dd, J = 8.1, 4.3 Hz, 1H), 7.68 – 7.57 (m, 7H), 7.44 – 7.30 (m, 6H), 7.23 (dd, J = 7.5, 0.9 Hz, 2H), 7.21 – 7.18 (m, 3H), 7.11 (d, J = 8.9 Hz, 2H), 6.06 (d, J = 14.3 Hz, 2H), 3.52 (s, 6H), 2.70 (t, J = 6.1 Hz, 4H), 2.03 – 1.97 (m, 2H), 1.30 (s, 12H).

^{13}C NMR (101 MHz, CD$_3$CN) δ (ppm): 173.9, 163.7, 161.3, 152.6, 149.5, 148.5, 145.6, 144.1, 142.2, 142.1, 139.1, 136.7, 132.5, 131.6, 131.4, 130.8, 129.9, 129.6, 128.7, 128.2, 126.0, 125.6, 124.6, 123.3, 123.2, 122.5, 121.0, 115.5, 111.8, 101.1, 49.9, 32.1, 27.9, 24.9, 21.9.

HRMS (ESI-TOF) *m/z* [M]$^+$ calcd for $C_{57}H_{51}N_6O$ 835.4119, found 835.4122.

Compound 11.

To a stirred solution of compound **9** (135 mg, 0.34 mmol) in anhydrous DMF (10 mL), under a N_2 atmosphere, was added NaH (15 mg, 0.34 mmol). After stirring for 10 min at room temperature, a solution of compound **8** (290 mg, 0.34 mmol) in anhydrous DMF (5 mL) was added dropwise and the resulting mixture was stirred for another 24 h at room temperature under a N_2 atmosphere. The solvent was removed *in vacuo* and the crude mixture was purified by column chromatography (silica gel, 0-20% MeOH in DCM) to afford compound **11** (95 mg, 32 % yield) as a dark blue solid.

TLC: R_f (10 % MeOH in DCM) 0.10.

¹H NMR (500 MHz, CD₃CN) δ 9.10 (dd, J = 4.4, 1.8 Hz, 1H), 9.03 (dd, J = 8.1, 1.8 Hz, 1H), 8.94 (dd, J = 4.2, 1.8 Hz, 1H), 7.84 – 7.79 (m, 3H), 7.75 – 7.70 (m, 4H), 7.67 – 7.55 (m, 8H), 7.45 (d, J = 8.8 Hz, 1H), 7.37 (d, J = 1.8 Hz, 1H), 7.35 (d, J = 4.2 Hz, 1H), 6.99 (dd, J = 8.4, 0.5 Hz, 2H), 6.04 (d, J = 14.3 Hz, 2H), 3.47 (s, 6H), 2.69 (t, J = 6.1 Hz, 4H), 2.01 – 1.97 (m, 2H), 1.28 (s, 12H).

¹³C NMR (126 MHz, CD₃CN) δ 173.2, 164.1, 161.2, 149.5, 148.5, 144.4, 144.1, 142.4, 138.4, 132.4, 132.2, 131.9, 131.5, 131.4, 131.3, 130.8, 129.9, 128.7, 124.6, 123.3, 116.0, 115.5, 113.7, 101.4, 88.6, 49.8, 32.1, 27.7, 24.8, 21.8.

HRMS (ESI-TOF) m/z [M]$^+$ calcd for $C_{57}H_{49}I_2N_6O$ 1087.2052, found 1087.2050.

Synthesis, and Characterization of Ru(II)-Cyanine complexes (1-3)

Compound Ru-Cyn-1.

A solution of [Ru(Bpy)₂Cl₂] (50 mg, 0.105 mmol) and compound **10** (100 mg, 0.126 mmol) in a 1:1 mixture of ethanol/water (10 mL) was stirred for 15 h at 70 ºC under a N₂ atmosphere. After cooling to room temperature, saturated aq. KPF₆ (2 mL) was added and the resulting precipitate was collected by filtration and washed thoroughly with water, acetone, and Et₂O. The crude was purified by column chromatography (silica gel, 0-7% MeOH in DCM) to give compound **Ru-Cyn-1** (60 mg, 45 % yield) as a dark green solid. The Cl⁻ salt was obtained by stirring a solution of the PF₆⁻ salt of the compound in HPLC-grade MeOH containing an excess of AmberLite™ IRA-410 Cl ion exchange resin during 15 h at room temperature.

TLC: R$_f$ (10 % MeOH in DCM): 0.25.

¹H NMR (400 MHz, CD₃CN) δ 9.14 (dd, J = 8.3, 1.3 Hz, 1H), 8.54 (dt, J = 8.1, 1.0 Hz, 1H), 8.54 – 8.48 (m, 2H), 8.49 – 8.46 (m, 1H), 8.10 – 8.06 (m, 2H), 8.02 – 7.97 (m, 2H), 7.91 (dd, J = 5.2, 1.3 Hz, 1H), 7.86 – 7.80 (m, 5H), 7.72 – 7.58 (m, 8H), 7.54 (ddd, J = 5.7, 1.5, 0.8 Hz, 1H), 7.47 – 7.43 (m, 2H), 7.41 – 7.36 (m, 6H), 7.24 – 7.21 (m, 6H), 7.15 (d, J = 9.0 Hz, 2H), 7.12 (d, J = 8.9 Hz, 1H), 6.07 (dd, J = 14.3, 2.4 Hz, 2H), 3.53 (s, 6H), 2.71 (t, J = 6.2 Hz, 4H), 2.04 – 1.98 (m, 2H), 1.30 (s, 12H).

¹³C NMR (101 MHz, CD₃CN) δ (ppm): 173.9, 163.5, 161.8, 158.1, 152.8, 151.8, 151.0, 144.1, 142.1, 138.9, 138.7, 132.7, 132.5, 132.0, 131.7, 131.6, 129.9, 129.6, 128.6, 128.4, 127.4, 126.3, 126.0, 125.3, 125.2, 123.1, 122.4, 115.8, 111.8, 101.2, 49.9, 32.1, 27.9, 24.9, 21.9.

HRMS (ESI-TOF) m/z [M]$^{3+}$ calcd for $C_{77}H_{67}N_{10}ORu$ 416.4842, found 416.4846.

Anal. Calcd for $C_{77}H_{67}N_{10}ORu(3Cl)(3.5H_2O)$: C, 64.93; H, 5.45; N, 9.71; Found: C 64.89; H 5.67; N 8.99.

Compound Ru-Cyn-2.

A solution of $[Ru(Bpy)_2Cl_2]$ (30 mg, 0.069 mmol) and compound **11** (75 mg, 0.115 mmol) in a 1:1 mixture of ethanol/water (10 mL) was stirred for 15 h at 70 ºC under a N_2 atmosphere. After cooling to room temperature, saturated aq. KPF_6 (2 mL) was added and the resulting precipitate was collected by filtration and washed thoroughly with water, acetone, and Et_2O. The crude was purified by column chromatography (silica gel, 0-10% MeOH in DCM) to give compound **Ru-Cyn-2** (56 mg, 32 % yield) as a dark green solid. The Cl⁻ salt was obtained by stirring a solution of the PF_6^- salt in HPLC-grade MeOH containing an excess of AmberLite™ IRA-410 Cl ion exchange resin during 15 h at room temperature.

TLC: R_f (10 % MeOH in DCM): 0.30.

¹H NMR (400 MHz, CD₃CN) δ 9.12 (dd, J = 8.2, 1.4 Hz, 1H), 8.52 (d, J = 8.3 Hz, 1H), 8.48 (dd, J = 8.2, 2.8 Hz, 2H), 8.45 (d, J = 8.2 Hz, 1H), 8.07 – 8.04 (m, 2H), 8.00 – 7.93 (m, 2H), 7.88 (dd, J = 5.2, 1.3 Hz, 1H), 7.81 – 7.77 (m, 4H), 7.72 – 7.69 (m, 4H), 7.67 – 7.63 (m, 3H), 7.63 – 7.59 (m, 2H), 7.59 – 7.54 (m, 4H), 7.53 – 7.49 (m, 1H), 7.45 – 7.38 (m, 3H), 7.34 (d, J = 5.2 Hz, 1H), 7.22 – 7.17 (m, 2H), 7.11 (d, J = 8.9 Hz, 2H), 6.97 (d, J = 9.1 Hz, 2H), 6.03 (d, J = 14.2 Hz, 2H), 3.45 (s, 6H), 2.67 (t, J = 6.2 Hz, 4H), 2.04 – 1.94 (m, 2H), 1.25 (s, 12H).

¹³C NMR (101 MHz, CD₃CN) δ (ppm): 173.2, 158.0, 152.7, 144.4, 144.1, 142.3, 138.8, 138.7, 138.4, 132.7, 132.2, 131.9, 129.4, 128.5, 128.3, 125.2, 125.1, 123.3, 115.7, 113.8, 101.5, 88.6, 49.7, 32.1, 27.7, 24.8, 21.7.

HRMS (ESI-TOF) *m/z* [M]³⁺ calcd for $C_{77}H_{65}I_2N_{10}ORu$ 500.4153, found 500.4165.

Compound Ru-Cyn-3.

A solution of $[Ru(Bphen)_2Cl_2]$ (30 mg, 0.036 mmol) and compound **10** (45 mg, 0.043 mmol) in a 1:1 mixture of ethanol/water (8 mL) was stirred for 15 h at 70 ºC under a N_2 atmosphere. After cooling to room temperature, saturated aq. KPF_6 (2 mL) was added and the resulting precipitate was collected by filtration and washed thoroughly with water, acetone, and Et_2O. The crude was purified by column chromatography (silica gel, 0-10% MeOH in DCM) to give compound **Ru-Cyn-3** (56 mg, 45 % yield) as a dark green solid. The Cl⁻ salt was obtained by stirring a solution of the PF_6^- salt in HPLC-grade MeOH containing an excess of AmberLite™ IRA-410 Cl ion exchange resin during 15 h at room temperature.

TLC: R_f (10 % MeOH in DCM): 0.32.

¹H NMR (400 MHz, CD₃CN) δ 9.07 (dd, J = 8.3, 1.3 Hz, 1H), 8.14 (d, J = 5.5 Hz, 1H), 8.12 (d, J = 1.3 Hz, 1H), 8.12 – 8.10 (m, 4H), 8.09 – 8.08 (m, 2H), 8.07 (d, J = 5.5 Hz, 1H), 8.02 (d, J = 5.5 Hz, 1H), 7.95 (dd, J = 5.3, 1.2 Hz, 1H), 7.74 (d, J = 14.3 Hz, 2H), 7.70 (dd, J = 8.3, 5.3 Hz, 1H), 7.63 – 7.58 (m, 2H), 7.58 – 7.45 (m, 30H), 7.37 (dd, J = 8.7, 1.2 Hz, 1H), 7.30 (d, J = 7.9 Hz, 2H), 7.24 (dd, J = 8.7, 5.3 Hz, 1H), 7.15 – 7.09 (m, 4H), 7.06 (d, J = 9.0 Hz, 2H), 5.97 (d, J = 14.3 Hz, 2H), 3.42 (s, 6H), 2.61 (t, J = 6.1 Hz, 4H), 1.94 – 1.88 (m, 2H), 1.20 (s, 12H).

¹³C NMR (101 MHz, CD₃CN) δ (ppm): 173.8, 163.4, 161.7, 154.6, 153.2, 152.1, 150.0, 149.4, 149.3, 147.2, 147.1, 142.0, 137.7, 136.6, 132.7, 131.9, 131.6, 130.7, 130.7, 130.6, 130.0, 129.9, 129.6, 129.5, 129.1, 127.2, 126.1, 125.9, 124.6, 123.0, 115.7, 111.7, 101.1, 49.8, 27.8, 24.8, 21.8.

HRMS (ESI-TOF) *m/z* [M]³⁺ calcd for $C_{105}H_{83}N_{10}ORu$ 533.8593 found 533.8602.

Compound Ru.

A solution of [Ru(Bpy)₂Cl₂] (100 mg, 0.206 mmol) and compound **9** (96 mg, 0.245 mmol) in a 1:1 mixture of ethanol/water (12 mL) was stirred for 15 h at 70 ºC under a N₂ atmosphere. After cooling to room temperature, saturated aq. KPF₆ (10 mL) was added and the resulting precipitate was collected by filtration and washed thoroughly with water and Et₂O to afford **Ru** (56 mg, 45 % yield) as a bright orange solid that did not require any further purification. The Cl⁻ salt was obtained by stirring a solution of the PF₆⁻ salt in HPLC-grade MeOH containing an excess of AmberLite™ IRA-410 Cl ion exchange resin during 15 h at room temperature.

¹H NMR (500 MHz, CD₃CN) δ 9.14 (dd, J = 8.4, 1.4 Hz, 1H), 8.59 (ddt, J = 18.0, 9.2, 4.8 Hz, 4H), 8.14 – 8.09 (m, 1H), 8.08 – 8.05 (m, 2H), 8.03 – 7.96 (m, 2H), 7.90 (dd, J = 5.2, 1.2 Hz, 1H), 7.85 (ddd, J = 5.6, 1.5, 0.7 Hz, 1H), 7.83 – 7.77 (m, 2H), 7.77 – 7.67 (m, 3H), 7.63 – 7.58 (m, 3H), 7.56 (ddd, J = 5.6, 1.5, 0.7 Hz, 1H), 7.51 (dd, J = 8.6, 1.2 Hz, 1H), 7.48 – 7.45 (m, 1H), 7.45 – 7.40 (m, 3H), 7.36 (dd, J = 8.6, 5.2 Hz, 1H), 7.26 – 7.16 (m, 2H), 6.96 (d, J = 8.8 Hz, 2H).

¹³C NMR (126 MHz, CD₃CN) δ 161.3, 158.2, 158.2, 158.0, 156.1, 152.9, 152.8, 152.8, 151.6, 150.7, 146.7, 138.8, 138.8, 138.7, 138.7, 138.4, 137.8, 131.8, 129.7, 129.6, 129.4, 128.5, 128.4, 128.4, 127.2, 127.0, 126.2, 125.4, 125.3, 123.1, 120.5, 116.6, 116.3, 49.8, 1.3.

HRMS (ESI-TOF) *m/z* [M]²⁺ calcd for $C_{45}H_{32}N_8ORu$ 401.0866, found 401.0875.

Cell culture

<u>Normoxia.</u> CT-26 cells were cultured in DMEM medium (Gibco, Life Technologies, USA) supplemented with 10 % of fetal calf serum (Gibco). A2780 cells were cultured in RPMI medium (Gibco) supplemented with 10 % of fetal calf serum. HT-29 cells were cultured in McCoy's 5A medium (Gibco) supplemented with 10 % of fetal calf serum. All cell lines were complemented with 1% penicillin-streptomycin mixture (Gibco) and maintained in a humidified atmosphere at 37 °C and 5 % of CO_2.

<u>Hypoxia.</u> CT-26 cells were cultured in DMEM medium (Gibco, Life Technologies, USA) supplemented with 10 % of fetal bovine serum (Gibco) and complemented with 1% penicillin-streptomycin mixture (Gibco) and maintained in an humidified atmosphere at 37 °C, 5 % of CO_2 and 2% O_2.

Photocytoxicity studies

<u>Normoxia.</u> Cells were seeded at a density of 4,000 cells/well in 96-well plates (100 µL/well) and were incubated at 37 °C, 5% CO_2 for 24 h. The medium was replaced by test compound dilutions in fresh medium (100 µL/well) from a 10 mM stock solution in DMSO and cells were incubated at 37 °C, 5% CO_2 for 4 h. The medium was replaced by 100 µL of fresh medium. Plates were then irradiated at the corresponding wavelength for 1 h using a LUMOS-BIO LED photoreactor (Atlas Photonics). As a control, a plate was kept in the dark for the same amount of time at 37°C, 0% CO_2. Cells were then incubated for an additional 44 h at 37 °C, 5% CO_2. The medium was replaced with 100 µL of fresh medium containing resazurin (0.2 mg/mL). After 4 h of incubation at 37 °C, 5% CO_2, plates were read using a Cytation 5 Microplate Reader (λ_{exc} = 540 nm; λ_{read} = 590 nm). Fluorescence data were normalized and fitted using GraphPad Prism Software and IC_{50} values were calculated by non-linear regression (sigmoidal dose-response curve with variable slope function).

<u>Hypoxia.</u> Cells were seeded at a density of 2,500 cells/well in 96-well plates (100 µL/well) and were incubated at 37 °C, 5% CO_2, 2% O_2 for 65 h. The medium used for dilutions (DMEM, Gibco, Life Technologies, USA) was deaerated in the hypoxia incubator (37 °C, 5% CO_2, 2% O_2) for 65 h before incubation. The medium in the plates was replaced by test compound dilutions in deareated DMEM (100 µL/well) from a 10 mM stock solution in DMSO and cells were incubated at 37 °C, 5% CO_2, 2% O_2 for 4 h. The medium was replaced by 100 µL of fresh deaerated medium. After 30 min of incubation at 2% O_2, plates were irradiated at 740 nm for 1 h using a LUMOS-BIO LED photoreactor (Atlas Photonics) in a hypoxia chamber (Plas labs 856-Series hypoxia chamber glove box, 2% O_2). (Figure S15) As a control, plates were kept in

22

the dark for the same amount of time at 37 °C, 5% CO_2, 2% O_2. Cells were then incubated for an additional 44 h at 37 °C, 5% CO_2, 2% O_2. The medium was replaced with 100 µL of fresh medium containing resazurin (0.2 mg/mL). After 4 h of incubation at 37 °C, 5% CO_2, 20% O_2, plates were read using a Cytation 5 Microplate Reader (λ_{exc} = 540 nm; λ_{read} = 590 nm). Fluorescence data were normalized and fitted using GraphPad Prism Software and IC_{50} values were calculated by non-linear regression (sigmoidal dose-response curve with variable slope function).

ICP-MS cellular uptake studies

CT-26 cells were seeded in a 6-cm cell culture dish at a density of $1x10^6$ cells/dish and were incubated at 37 °C, 5% CO_2 for 24 h. The medium was replaced with 1 mL of a 10-µM dilution of the Ru(II)-complexes in fresh DMEM from a 10 mM stock solution in DMSO and cells were incubated at 37 °C, 5% CO_2 for 4 h. After trypsinization, cells were collected, counted, and stored at – 80 °C. ICP-MS samples were prepared as follows: samples were digested using 70% nitric acid (1 mL, 60 °C, overnight) and then further diluted 1:100 (1% HCl solution in MQ water) and analyzed using ICP-MS. All ICP-MS measurements were performed on an Agilent 7900 Quadrupole ICP-MS located at the Institut de Physique du Globe de Paris (France). The monitored Ruthenium isotopes are 99 and 101. Throughout the course of the analytical sequence, an indium internal standard was injected after inline mixing with the samples to correct for signal drift and matrix effects. A set of calibration standards were analyzed to confirm and model (through simple linear regression) the linear relationship between signal and concentration. The model was then used to convert measured sample counts to concentrations. Reported uncertainties were calculated using error propagation equations and considering the combination of standard deviation on replicated consecutive signal acquisitions (n=3), internal-standard ratio, and blank subtraction. The non-linear term (internal-standard ratio) was linearized using a first-order Taylor series expansion to simplify error propagation. The amount of metal detected in the cell samples was transformed from ppb to µg of metal. Data were normalized to the number of cells and expressed as µmol of metal/number of cells.

Subcellular Localization by Fluorescence Microscopy

HeLa cells were maintained in Dulbecco's modified Eagle's medium (DMEM) containing high glucose (4.5 g/L) and supplemented with 10% fetal bovine serum (FBS) and 50 U/mL penicillin–streptomycin. For cellular uptake experiments and posterior observation under a

microscope, cells were seeded on glass-bottom dishes (P35G-1.5-14-C, Mattek) and incubated overnight at 37 °C, 5% CO_2. The next day the culture medium was replaced with 10 μM dilutions of the complexes in DMEM complete medium and the dishes were incubated for 1 hours at 37 °C, 5% CO_2. In colocalization experiments, cells were washed after the incubation time with the compounds and incubated for 30 min at 37 °C, 5% CO_2 with MitoTracker Green (Invitrogen ™) at 0.1 μM in non-complemented DMEM.

Cells were washed with DPBS and imaged in phenol red-free DMEM with Hepes (10mM) on a Leica Thunder fluorescence microscope (Leica Microsystems) equipped with a x63/1.40 plan apochromat oil objective. The excitation and emission filters were: Exc 479/33 Em 519/25 together with a 475 nm LED for the MTG staining and Exc 730/40 Em 810/80 with a 730 nm LED for the compounds. Images were first deconvolved with the Small Volume Computational Clearing (SVCC) algorithm of the Leica Thunder microscope (Leica Microsystems) and then processed and analyzed with Fiji[62]. For the colocalization studies the MitoTracker and compound channels were processed by median filtering (radius = 1) and background subtraction (rolling ball radius = 30). Colocalization coefficients were measured using the JaCoP plugin[63] on the different stacks of images (more than 50 cells for each experiment) setting the thresholds for the compound and MTG channels based on the Otsu threshold clustering algorithm[64].

Conflicts of interest

The authors declare no competing financial interests.

Supporting information.

The authors have cited additional references within the Supporting Information.[65-68]

References

[1]   B. P. Cabral, M. da G. D. Fonseca, F. B. Mota, *Oncotarget* **2018**, *9*, 30474–30484.

[2]   Z. Wang, Z. Deng, G. Zhu, *Dalt. Trans.* **2019**, *48*, 2536–2544.

[3]   A.-M. Florea, D. Büsselberg, *Cancers (Basel).* **2011**, *3*, 1351–1371.

[4]   N. Vasan, J. Baselga, D. M. Hyman, *Nature* **2019**, *575*, 299–309.

[5]   C. Mari, V. Pierroz, S. Ferrari, G. Gasser, *Chem. Sci.* **2015**, *6*, 2660–2686.

[6]   X. Zhao, J. Liu, J. Fan, H. Chao, X. Peng, *Chem. Soc. Rev.* **2021**, *50*, 4185–4219.

[7]   L. Conti, E. Macedi, C. Giorgi, B. Valtancoli, V. Fusi, *Coord. Chem. Rev.* **2022**, *469*, 214656.

[8]   S. Monro, K. L. Colón, H. Yin, J. Roque, P. Konda, S. Gujar, R. P. Thummel, L. Lilge, C. G. Cameron, S. A. McFarland, *Chem. Rev.* **2019**, *119*, 797–828.

[9]   M. Ankathatti Munegowda, A. Manalac, M. Weersink, S. A. McFarland, L. Lilge, *Coord. Chem. Rev.* **2022**, *470*, 214712.

[10]   S. A. McFarland, A. Mandel, R. Dumoulin-White, G. Gasser, *Curr. Opin. Chem. Biol.* **2020**, *56*, 23–27.

[11]   A. Gandioso, K. Purkait, G. Gasser, *Chimia (Aarau).* **2021**, *75*, 845–855.

[12]   A. Mani, T. Feng, A. Gandioso, R. Vinck, A. Notaro, L. Gourdon, P. Burckel, B. Saubaméa, O. Blacque, K. Cariou, J.-E. Belgaied, H. Chao, G. Gasser, *Angew. Chemie* **2023**, DOI 10.1002/ange.202218347.

[13]   S. Lazic, P. Kaspler, G. Shi, S. Monro, T. Sainuddin, S. Forward, K. Kasimova, R. Hennigar, A. Mandel, S. McFarland, L. Lilge, *Photochem. Photobiol.* **2017**, *93*, 1248–1258.

[14]   P. Zhang, Y. Wang, K. Qiu, Z. Zhao, R. Hu, C. He, Q. Zhang, H. Chao, *Chem. Commun.* **2017**, *53*, 12341–12344.

[15]   R. Weissleder, *Nat. Biotechnol.* **2001**, *19*, 316–317.

[16]   J. B. Grimm, L. D. Lavis, *Nat. Methods* **2022**, *19*, 149–158.

[17]   J. Shen, W. He, *Coord. Chem. Rev.* **2023**, *483*, 215096.

[18]   F. Schmitt, N. P. E. Barry, L. Juillerat-Jeanneret, B. Therrien, *Bioorg. Med. Chem. Lett.* **2012**, *22*, 178–180.

[19]   L. M. Lifshits, J. A. Roque III, P. Konda, S. Monro, H. D. Cole, D. von Dohlen, S. Kim, G. Deep, R. P. Thummel, C. G. Cameron, S. Gujar, S. A. McFarland, *Chem. Sci.* **2020**, *11*, 11740–11762.

[20]   P. Konda, J. A. Roque III, L. M. Lifshits, A. Alcos, E. Azzam, G. Shi, C. G. Cameron,

S. A. McFarland, S. Gujar, *Am J Cancer Res* **2022**, *12*, 210–228.

[21] M. Martínez-Alonso, A. Gandioso, C. Thibaudeau, X. Qin, P. Arnoux, N. Demeubayeva, V. Guérineau, C. Frochot, A. C. Jung, C. Gaiddon, G. Gasser, *ChemBioChem* **2023**, e202300203.

[22] Y. Xie, B. Killinger, A. Moszczynska, O. Merkel, *Molecules* **2016**, *21*, 1334.

[23] F. Heinemann, J. Karges, G. Gasser, *Acc. Chem. Res.* **2017**, *50*, 2727–2736.

[24] P. L. Choyke, R. Alford, H. M. Simpson, J. Duberman, G. Craig Hill, M. Ogawa, C. Regino, H. Kobayashi, *Mol. Imaging* **2009**, *8*, 341–354.

[25] Q. Zheng, M. F. Juette, S. Jockusch, M. R. Wasserman, Z. Zhou, R. B. Altman, S. C. Blanchard, *Chem. Soc. Rev.* **2014**, *43*, 1044–1056.

[26] B. Bertrand, K. Passador, C. Goze, F. Denat, E. Bodio, M. Salmain, *Coord. Chem. Rev.* **2018**, *358*, 108–124.

[27] V. Novohradsky, A. Rovira, C. Hally, A. Galindo, G. Vigueras, A. Gandioso, M. Svitelova, R. Bresolí-Obach, H. Kostrhunova, L. Markova, J. Kasparkova, S. Nonell, J. Ruiz, V. Brabec, V. Marchán, *Angew. Chemie - Int. Ed.* **2019**, *58*, 6311–6315.

[28] Q. Yang, H. Jin, Y. Gao, J. Lin, H. Yang, S. Yang, *ACS Appl. Mater. Interfaces* **2019**, *11*, 15417–15425.

[29] W. Zhang, Y. Liu, Q. Gao, C. Liu, B. Song, R. Zhang, J. Yuan, *Chem. Commun.* **2018**, *54*, 13698–13701.

[30] Y. Wu, J. Wu, W.-Y. Wong, *Biomater. Sci.* **2021**, *9*, 4843–4853.

[31] A. P. Gorka, R. R. Nani, M. J. Schnermann, *Acc. Chem. Res.* **2018**, *51*, 3226–3235.

[32] G. Fei, S. Ma, C. Wang, T. Chen, Y. Li, Y. Liu, B. Tang, T. D. James, G. Chen, *Coord. Chem. Rev.* **2021**, *447*, 214134.

[33] G. S. Gopika, P. M. H. Prasad, A. G. Lekshmi, S. Lekshmypriya, S. Sreesaila, C. Arunima, M. S. Kumar, A. Anil, A. Sreekumar, Z. S. Pillai, *Mater. Today Proc.* **2020**, *46*, 3102–3108.

[34] E. M. S. Stennett, M. A. Ciuba, M. Levitus, *Chem. Soc. Rev.* **2014**, *43*, 1057–1075.

[35] X. Zhao, Q. Yao, S. Long, W. Chi, Y. Yang, D. Tan, X. Liu, H. Huang, W. Sun, J. Du, J. Fan, X. Peng, *J. Am. Chem. Soc.* **2021**, *143*, 12345–12354.

[36] O. Semenova, D. Kobzev, F. Yazbak, F. Nakonechny, O. Kolosova, A. Tatarets, G. Gellerman, L. Patsenker, *Dye. Pigment.* **2021**, *195*, 109745.

[37] A. Gandioso, A. Vidal, P. Burckel, G. Gasser, E. Alessio, *ChemBioChem* **2022**, *23*, DOI 10.1002/cbic.202200398.

[38] J. Atchison, S. Kamila, H. Nesbitt, K. A. Logan, D. M. Nicholas, C. Fowley, J. Davis,

B. Callan, A. P. McHale, J. F. Callan, *Chem. Commun.* **2017**, *53*, 2009–2012.

[39] J. H. Flanagan, S. H. Khan, S. Menchen, S. A. Soper, R. P. Hammer, *Bioconjug. Chem.* **1997**, *8*, 751–756.

[40] C. Ornelas, R. Lodescar, A. Durandin, J. W. Canary, R. Pennell, L. F. Liebes, M. Weck, *Chem. - A Eur. J.* **2011**, *17*, 3619–3629.

[41] J. Liu, Y. Chen, G. Li, P. Zhang, C. Jin, L. Zeng, L. Ji, H. Chao, *Biomaterials* **2015**, *56*, 140–153.

[42] C. Tanielian, C. Wolff, M. Esch, *J. Phys. Chem.* **1996**, *100*, 6555–6560.

[43] L. Strekowski, M. Lipowska, G. Patonay, *J. Org. Chem.* **1992**, *57*, 4578–4580.

[44] I. Bratsos, E. Alessio, in *Inorg. Synth.* (Eds.: M.E. Ringenberg, T.B. Rauchfuss), John Wiley & Sons, Inc., Hoboken, NJ, USA, **2010**, pp. 148–163.

[45] H. Ishida, S. Tobita, Y. Hasegawa, R. Katoh, K. Nozaki, *Coord. Chem. Rev.* **2010**, *254*, 2449–2458.

[46] E. A. Steck, A. R. Day, *J. Am. Chem. Soc.* **1943**, *65*, 452–456.

[47] G. Ghosh, H. Yin, S. M. A. Monro, T. Sainuddin, L. Lapoot, A. Greer, S. A. McFarland, *Photochem. Photobiol.* **2020**, *96*, 349–357.

[48] M. P. Luciano, S. N. Crooke, S. Nourian, I. Dingle, R. R. Nani, G. Kline, N. L. Patel, C. M. Robinson, S. Difilippantonio, J. D. Kalen, M. G. Finn, M. J. Schnermann, *ACS Chem. Biol.* **2019**, *14*, 934–940.

[49] A. R. Nödling, E. M. Mills, X. Li, D. Cardella, E. J. Sayers, S.-H. Wu, A. T. Jones, L. Y. P. Luk, Y.-H. Tsai, *Chem. Commun.* **2020**, *56*, 4672–4675.

[50] E. Ortega-Forte, A. Rovira, A. Gandioso, J. Bonelli, M. Bosch, J. Ruiz, V. Marchán, *J. Med. Chem.* **2021**, *64*, 17209–17220.

[51] M. D. Yaqoob, L. Xu, C. Li, M. M. L. Leong, D. D. Xu, *Photodiagnosis Photodyn. Ther.* **2022**, *38*, 102830.

[52] B. Myrzakhmetov, P. Arnoux, S. Mordon, S. Acherar, I. Tsoy, C. Frochot, *Pharmaceuticals* **2021**, *14*, 1–21.

[53] E. Ortega-Forte, A. Rovira, M. López-Corrales, A. Hernández-García, F. J. Ballester, E. Izquierdo-García, M. Jordà-Redondo, M. Bosch, S. Nonell, M. D. Santana, J. Ruiz, V. Marchán, G. Gasser, *Chem. Sci.* **2023**, *14*, 7170–7184.

[54] W. Sun, Y. Wen, R. Thiramanas, M. Chen, J. Han, N. Gong, M. Wagner, S. Jiang, M. S. Meijer, S. Bonnet, H. J. Butt, V. Mailänder, X. J. Liang, S. Wu, *Adv. Funct. Mater.* **2018**, *28*, DOI 10.1002/adfm.201804227.

[55] L. N. Lameijer, D. Ernst, S. L. Hopkins, M. S. Meijer, S. H. C. Askes, S. E. Le

Dévédec, S. Bonnet, *Angew. Chemie - Int. Ed.* **2017**, *56*, 11549–11553.

[56] G. Vigueras, L. Markova, V. Novohradsky, A. Marco, N. Cutillas, H. Kostrhunova, J. Kasparkova, J. Ruiz, V. Brabec, *Inorg. Chem. Front.* **2021**, *8*, 4696–4711.

[57] V. Novohradsky, L. Markova, H. Kostrhunova, J. Kasparkova, J. Ruiz, V. Marchán, V. Brabec, *Chem. - A Eur. J.* **2021**, *27*, 8547–8556.

[58] L. K. McKenzie, M. Flamme, P. S. Felder, J. Karges, F. Bonhomme, A. Gandioso, C. Malosse, G. Gasser, M. Hollenstein, *RSC Chem. Biol.* **2022**, *3*, 85–95.

[59] C. E. Mccusker, J. K. Mccusker, **2011**, 1656–1669.

[60] R. Dip, M. Otf, R. Caspar, C. Cordier, J. B. Waern, C. Guyard-duhayon, M. Gruselle, P. Le Floch, H. Amouri, **2006**, *45*, 58–62.

[61] T. M. Ebaston, F. Nakonechny, E. Talalai, G. Gellerman, L. Patsenker, *Dye. Pigment.* **2021**, *184*, 108854.

[62] J. Schindelin, I. Arganda-Carreras, E. Frise, V. Kaynig, M. Longair, T. Pietzsch, S. Preibisch, C. Rueden, S. Saalfeld, B. Schmid, J.-Y. Tinevez, D. J. White, V. Hartenstein, K. Eliceiri, P. Tomancak, A. Cardona, *Nat. Methods* **2012**, *9*, 676–682.

[63] S. Bolte, F. P. Cordelières, *J. Microsc.* **2006**, *224*, 213–232.

[64] N. Otsu, *IEEE Trans. Syst. Man. Cybern.* **1979**, *9*, 62–66.

[65] C. A. Bonda, S. Hu, J. Zhang, Z. Zhang, Compositions, Apparatus, Systems, and Methods for Resolving Electronic Excited States, **2014**, US 0044654 A1.

[66] S. Y. Park, M. Ebihara, Y. Kubota, K. Funabiki, M. Matsui, Dye. Pigment. **2009**, 82, 258–267.

[67] E. Ortega-Forte, A. Rovira, M. López-Corrales, A. Hernández-García, F. J. Ballester, E. Izquierdo-García, M. Jordà-Redondo, M. Bosch, S. Nonell, M. D. Santana, J. Ruiz, V. Marchán, G. Gasser, Chem. Sci., **2023**, 14, 7170–7184.

[68] M. Ankathatti Munegowda, A. Manalac, M. Weersink, S. A. McFarland, L. Lilge, Coord. Chem. Rev., **2022**, 470, 214712.